

## Research paper

The  $[\text{Rh}(\text{Xantphos})]^+$  catalyzed hydroboration of diphenylacetylene using trimethylamine-boraneMaximilian Dietz<sup>a,b</sup>, Alice Johnson<sup>a</sup>, Antonio Martínez-Martínez<sup>a</sup>, Andrew S. Weller<sup>a,\*</sup><sup>a</sup> Department of Chemistry, Chemistry Research Laboratories, University of Oxford, Oxford OX1 3TA, UK<sup>b</sup> Institut für Anorganische Chemie, Julius-Maximilians-Universität Würzburg, Am Hubland, D-97074 Würzburg, Germany

## ARTICLE INFO

## Keywords:

Rhodium  
Hydroboration  
Amine borane  
Mechanism

## ABSTRACT

The rhodium(I) complex  $[\text{Rh}(\kappa^3\text{-P,O,P-Xantphos})(\eta^2\text{-PhC}\equiv\text{CPh})][\text{BAR}_4^{\text{F}}]$  ( $\text{Ar}^{\text{F}} = 3,5\text{-(CF}_3)_2\text{C}_6\text{H}_4$ ) is an effective catalyst for the *cis*-selective hydroboration of the alkyne diphenylacetylene using the amine-borane  $\text{H}_3\text{B-NMe}_3$ . Detailed mechanistic studies, that include initial rate measurements, full simulation of temporal profiles for a variety of catalyst and substrate concentrations, and speciation experiments, suggest a mechanism that involves initial coordination of alkyne and a saturation kinetics regime for amine-borane binding. The solid-state molecular structure of a model complex that probes the proposed resting state is also reported,  $[\text{Rh}(\kappa^3\text{-P,O,P-Xantphos})(\text{NCMe})(\eta^2\text{-PhC}\equiv\text{CPh})][\text{BAR}_4^{\text{F}}]$ .

## 1. Introduction

The transition metal catalyzed hydroboration or diboration of carbon-carbon multiple bonds using three-coordinate boron containing reagents such as  $\text{HBcat}$  or  $\text{pin}_2\text{B}_2$  (cat = catechol, pin = pinacol) is an important methodology in organic synthesis as the corresponding organoboranes [1–3], can be functionalized to give products useful in organic and materials synthesis. Examples of hydroboration strategies that use stable four-coordinate boranes are less well established, e.g.  $\text{H}_3\text{B-L}$  (L = Lewis base) [4,5], despite the potential advantages in air-stability and handling that such reagents offer compared to three coordinate borane reagents, or more traditional reagents such as  $\text{H}_3\text{B-THF}$ . We have previously reported that  $[\text{Rh}(\kappa^2\text{-P,P-Xantphos})(\eta^2,\eta^2\text{-H}_2\text{B}(\text{NMe}_3)\text{CH}_2\text{CH}_2^t\text{Bu})][\text{BAR}_4^{\text{F}}]$ , **I**, (Xantphos = 4,5-bis(diphenylphosphino)-9,9-dimethylxathene,  $\text{Ar}^{\text{F}} = 3,5\text{-(CF}_3)_2\text{C}_6\text{H}_4$ , Scheme 1) is an effective catalyst for the hydroboration of the hindered terminal alkene tert-butyl ethene (TBE) using  $\text{H}_3\text{B-NMe}_3$ , to give the linear (anti-Markovnikov) alkylborane product  $\text{H}_2\text{B}(\text{CH}_2\text{CH}_2^t\text{Bu})\cdot\text{NMe}_3$  [6]. Mechanistic studies showed that this transformation was competitive with a slower alkene-promoted B–B dehydrogenative homocoupling to give a strongly-bound, diborane(4),  $\text{H}_4\text{B}_2\cdot 2\text{NMe}_3$  complex,  $[\text{Rh}(\kappa^2\text{-P,P-Xantphos})(1,2\text{-}\eta^2\text{-}(\text{H}_2\text{BNMe}_3)_2)][\text{BAR}_4^{\text{F}}]$  **II** [7]; while binding of the hydroboration product also inhibits catalysis. We now report an extension of this strategy to report the *cis*-selective hydroboration of the internal alkyne,  $\text{PhC}\equiv\text{CPh}$ , using  $\text{H}_3\text{B-NMe}_3$  to give the vinyl borane,  $\text{PhCH}=\text{CPh}(\text{BH}_2\text{NMe}_3)$ , that is promoted by the readily accessible

pre-catalyst  $[\text{Rh}(\kappa^3\text{-P,O,P-Xantphos})(\eta^2\text{-PhC}\equiv\text{CPh})][\text{BAR}_4^{\text{F}}]$ , **1**. Complex **1** is also an active catalyst for the carbthiolation of terminal and internal alkynes [8,9]. A catalytic cycle is proposed based upon kinetic, resting state and isotope-labelling experiments, in conjunction with the synthesis and characterization of model complexes.

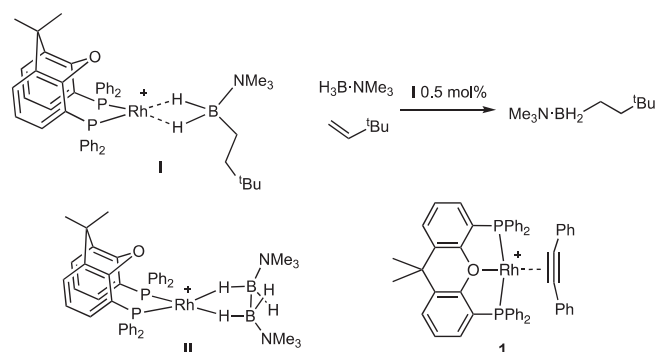
## 2. Results and discussion

The pre-catalyst complex **1** was prepared as reported previously [8]. Initial screening experiments, at 0.5 mol% catalyst loading, showed that this was an effective – if slow (48 h, unoptimized) – catalyst for the *cis*-hydroboration of diphenylacetylene to give the vinyl base-stabilized borane  $\text{PhCH}=\text{CPh}(\text{BH}_2\text{NMe}_3)$ , **2**, in greater than 95% spectroscopic yield, and 88% isolated yield (0.15 g) as colorless crystalline material, Fig. 1. The identity of **2** was ultimately resolved by a single crystal X-ray diffraction study that showed it to be the product of overall *cis*-addition of  $\text{H}_3\text{B-NMe}_3$  across the triple bond [ $\text{C}=\text{C}$ , 1.344(2),  $\text{C-B}$  1.614(2) Å]. In the  $^1\text{H}$  NMR spectrum of **2** the vinyl signal is observed at  $\delta$  6.80 (1 H relative integral) and the  $\text{NMe}_3$  groups at  $\delta$  2.42 (9H), the former characteristic of the vinyl group of hydroborated diphenylacetylene [10,11]. These two signals also show a strong correlation in the NOE-difference spectrum, consistent with *cis*-addition. In the  $^{11}\text{B}\{^1\text{H}\}$  NMR spectrum a single resonance is observed at  $\delta$  0.9, shifted 8.2 ppm downfield from  $\text{H}_3\text{B-NMe}_3$ , and is consistent with a four coordinate  $^{11}\text{B}$  environment.

With the identity of the product of catalysis identified as the *cis*-

\* Corresponding author.

E-mail address: [andrew.weller@chem.ox.ac.uk](mailto:andrew.weller@chem.ox.ac.uk) (A.S. Weller).



**Scheme 1.** Hydroboration of TBE using  $\text{H}_3\text{B-NMe}_3$ , catalyst **I**, the product of B–B dehydrogenative homocoupling, **II**, and catalyst **1**.  $[\text{BAr}_4^F]^-$  anions are not shown.

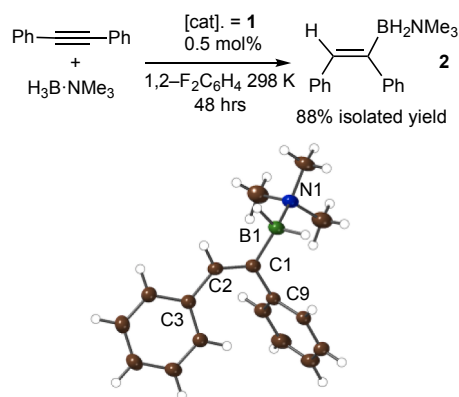


**Fig. 1.** Catalytic synthesis of **2** and its solid-state structure. Selected bond lengths (Å) and angles (°): C1–C2, 1.344(2); C1–B1, 1.614(2); B1–N1, 1.637(2); C2–C1–B1, 119.3(1); C3/C2/C1/C9 torsion = 7.3(2)°.

hydroborated product, the details of the mechanism were probed by combined kinetic and speciation studies. The 48 h reaction time to completion at 0.5 mol% of **1** was not suitable for kinetic studies using in situ NMR spectroscopic monitoring, so higher catalyst loadings were used (1–4 mol%). These conditions resulted in acceptable times to full completion of up to 3 h at 298 K at 1 mol%. Fig. 2A shows a representative set of time/concentration data for catalysis when  $[\mathbf{1}] = 2.5 \text{ mol\%}$ .

Working at the baseline conditions of  $[\text{PhC}\equiv\text{CPh}] = [\text{H}_3\text{B-NMe}_3] = 0.435 \text{ M}$ ,  $\mathbf{1} = 2.5 \text{ mol\%}$ , the progress of the reaction was monitored by  $^{11}\text{B}$  NMR spectroscopy by following the integrals of  $\text{H}_3\text{B-NMe}_3$  and product **2**, using  $[\text{BAr}_4^F]^-$  (from **1**) as an internal standard. Under these conditions the reaction followed a zero-order profile for the first ~75% of reaction, with some curvature (deceleration) at higher conversions. Initial rate measurements over the first 5% of turnover, in which concentrations of catalyst and substrates were independently varied, reveals that turnover is close to zero order in  $\text{H}_3\text{B-NMe}_3$ . The data do suggest that at lower concentrations of  $[\text{H}_3\text{B-NMe}_3]_0$  the initial rate drops slightly (Fig. 2B) – which may be related to the curvature seen at higher conversions, although the deviation from zero order is small. No such attenuation is observed on variation of  $\text{PhC}\equiv\text{CPh}$ , which shows a zero-order relationship (Fig. 2C). The reaction is first order in precatalyst, **1** (D). A KIE measurement using the initial rate method performed on Fig. 2 independent samples using  $\text{D}_3\text{B-NMe}_3$  (baseline concentration conditions) results in  $k_{\text{H}}/k_{\text{D}} = 1.4(1)$ . No product inhibition is observed, as addition of 10 or 20 equivalents of **2** to catalysis mixtures resulted in no appreciable change in temporal profile or overall conversion (Fig. 2A inset).

Overall these data suggest a saturation-kinetics model for  $\text{H}_3\text{B-NMe}_3$  binding, which follows on from an essentially irreversible binding of

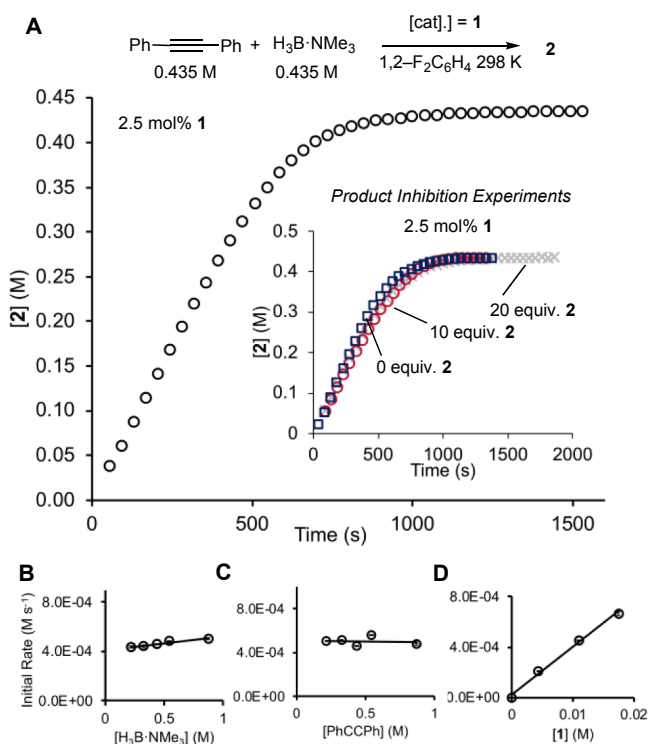


**Fig. 2.** A Time/concentration profile for the reaction between  $\text{H}_3\text{B-NMe}_3/\text{PhC}\equiv\text{CPh}$  catalyzed by **1** (0.0109 M, 2 mol%). Inset shows temporal profile when product **2** (0, 10 and 20 equivalents) is added to the initial solution. B–D Initial rates plots derived from the pseudo zero order regime (5% total turnover) B: variation of  $\text{H}_3\text{B-NMe}_3$ ,  $[\text{PhC}\equiv\text{CPh}] = 0.435 \text{ M}$ ,  $[\mathbf{1}] = 0.0109 \text{ M}$ , 2 mol%; C variation of  $\text{PhC}\equiv\text{CPh}$ ,  $[\text{H}_3\text{B-NMe}_3] = 0.435 \text{ M}$ ,  $[\mathbf{1}] = 0.0109 \text{ M}$ , 2 mol%; D variation of **1**,  $[\text{H}_3\text{B-NMe}_3]/[\text{PhC}\equiv\text{CPh}] = 0.435 \text{ M}$ .

alkyne and precedes the turnover-limiting step. Using these experimental observations, a holistic model was developed using COPASI [12], that combined multiple data sets where the concentrations of the reaction partners were varied. In the absence of specific measured rate constants this model only provides overall relative rates, rather than absolute values, and some consecutive individual steps were telescoped for simplicity and to avoid over-parametrization. Nevertheless, the simulation recreates the experimental data well (Fig. 3), and the model is consistent with: (i) strong – but reversible – binding of  $\text{H}_3\text{B-NMe}_3$  to **1**, (ii) a turnover limiting step that produces product (**2**) bound to the metal center and (iii) fast displacement of **2** by alkyne to reform **1**. The model predicts the steps involved in the turnover limiting process to have  $k_2 = 0.061(2) \text{ s}^{-1}$ , which compares favorably with the value that can be estimated from initial rate studies that give  $k_2(\text{obs}) = 0.052(4) \text{ s}^{-1}$ , which is calculated assuming an upper bound of  $[\mathbf{1-H}_3\text{B-NMe}_3] \leq [\text{Rh}]_{\text{TOT}}$ , an assumption which is not unreasonable given the saturation kinetics observed.

By following the reaction using  $^{31}\text{P}\{^1\text{H}\}$  NMR spectroscopy (2.5 mol% **1**,  $[\text{H}_3\text{B-NMe}_3] = [\text{PhC}\equiv\text{CPh}]$ , 1,2- $\text{F}_2\text{C}_6\text{H}_4$ ) the resting state was observed, as a broad doublet at  $\delta 27.9$  [ $J(\text{RhP}) = 114 \text{ Hz}$ ], that is distinct from **1** [ $\delta 20.4$ ,  $J(\text{RhP}) = 125 \text{ Hz}$ ]. The  $^{11}\text{B}$  NMR spectrum shows a very broad signal that is essentially unshifted from free  $\text{H}_3\text{B-NMe}_3$ . These data are consistent with  $\text{H}_3\text{B-NMe}_3$  binding to **1**, but in rapid equilibrium with unbound amine-borane. Evidence for a  $\eta$ -bound amine-borane comes from combination of **1** and 2 equivalents of  $\text{H}_3\text{B-NMe}_3$  in  $\text{CD}_2\text{Cl}_2$  measured at  $-60^\circ\text{C}$ . In this experiment a broad signal is observed at  $\delta 0.76$  [free  $\text{H}_3\text{B-NMe}_3$ ,  $\delta 2.27$ ] that sharpens in the  $^{11}\text{B}\{^1\text{H}\}$  NMR spectrum, suggestive of a time averaged  $\text{Rh}\cdots\text{H}_3\text{B}$  interaction. We thus propose  $[\text{Rh}(\kappa^3\text{-P,O,P-Xantphos})(\eta^1\text{-H}_3\text{B-NMe}_3)(\eta^2\text{-PhC}\equiv\text{CPh})][\text{BAr}_4^F]$  **3**, as the resting state (Scheme 2) in which amine-borane and alkyne are bound with the metal center. As formulated

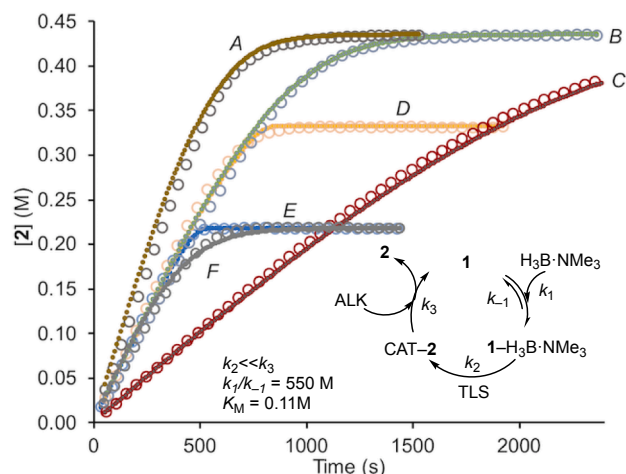


**Fig. 3.** Time/concentration profiles for a variety of starting concentrations of substrates and **1**. Solvent = 1,2- $\text{F}_2\text{C}_6\text{H}_4$ . Open circles = experimental data, dotted lines = holistically simulated data derived from the catalytic scheme shown in the inset using COPASI, CAT-2 = product bound complex. ALK =  $\text{PhC}\equiv\text{CPh}$ .  $K_M = (k_{-1} + k_2)/k_1$ . A–C:  $[\text{H}_3\text{B}\cdot\text{NMe}_3] = [\text{PhC}\equiv\text{CPh}] = 0.435\text{ M}$ ;  $[\text{Rh}]_{\text{TOT}} = 0.0174\text{ M}$ , 4 mol% (A); 0.0109 M, 2.5 mol% (B); 0.00435 M, 1 mol% (C); D:  $[\text{Rh}]_{\text{TOT}} = 0.0109\text{ M}$ , 3.3 mol%,  $\text{H}_3\text{B}\cdot\text{NMe}_3 = 0.435\text{ M}$ ,  $[\text{PhC}\equiv\text{CPh}] = 0.332\text{ M}$ ; E:  $[\text{Rh}]_{\text{TOT}} = 0.0109\text{ M}$ , 5 mol%,  $\text{H}_3\text{B}\cdot\text{NMe}_3 = 0.435\text{ M}$ ,  $[\text{PhC}\equiv\text{CPh}] = 0.2175\text{ M}$ ; F:  $[\text{Rh}]_{\text{TOT}} = 0.0145\text{ M}$ , 6.7 mol%,  $\text{H}_3\text{B}\cdot\text{NMe}_3 = 0.2175\text{ M}$ ,  $[\text{PhC}\equiv\text{CPh}] = 0.435\text{ M}$ .

complex **3** is an example of an 18-electron Rh(I) center with  $\text{Rh}\cdots\text{H}\cdots\text{B}$  interactions, for which there is precedent [13–15]. At the end of catalysis, the final organometallic product observed is dependent on the ratio of substrates. When alkyne is in excess, or there is a 1:1 ratio, complex **1** is observed. When  $\text{H}_3\text{B}\cdot\text{NMe}_3$  is in excess (i.e. 150 mol%, trace D Fig. 3) the homocoupled product, **II**, is the final organometallic product. As this is not a competent catalyst, but catalysis goes to completion under these conditions, we suggest **II** is formed only when alkyne is consumed, post productive turnover.

Further evidence for complex **3** being the resting state comes from addition of MeCN to the catalysis mixture at the early stages of turnover (10% conversion).  $^{31}\text{P}\{^1\text{H}\}$  NMR spectroscopy showed the immediate and quantitative formation of a new organometallic product [ $\delta$  27.4,  $J$  (RhP) = 115 Hz], while  $^{11}\text{B}$  NMR spectroscopy showed that the signal due to  $\text{H}_3\text{B}\cdot\text{NMe}_3$  had sharpened, suggesting displacement by MeCN. This  $^{31}\text{P}$  chemical shift is very similar to that observed for the resting state complex **3**. This new complex was a poor catalyst for the hydroboration reaction, promoting only 50% conversion after 24 h, demonstrating that MeCN largely outcompetes the  $\text{H}_3\text{B}\cdot\text{NMe}_3$  for binding to the metal center. The identity of this new species was resolved by a single crystal X-ray diffraction study on independently synthesized material, that comes from addition of MeCN to **1**. Fig. 4 shows the solid-state of the cation, which is a five coordinate Rh(I) complex  $[\text{Rh}(\kappa^3\text{-P}_2\text{O}_2\text{-Xantphos})(\text{NCMe})(\eta^2\text{-PhC}\equiv\text{CPh})][\text{BAR}_4^+]$ , **4**. The coordination geometry around the metal center is pseudo trigonal bipyramidal with the two phosphine groups in axial positions. The NCMe ligand has not displaced the alkyne, consistent with the kinetic model, and binds in the equatorial plane. Interestingly these  $^1\text{H}$  NMR data show a single

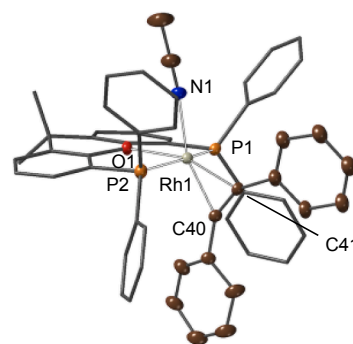


**Fig. 4.** Solid-state structure of the cationic portion of complex **4**. Selected bond lengths (Å) and angles (°): Rh1–P1, 2.2917(6); Rh1–P2, 2.2922(6); Rh1–O1, 2.2754(15); Rh1–N1, 2.152(2); Rh1–C40, 2.072(2); Rh1–C41, 2.050(2); C40–C41, 1.271(4); O1–Rh1–N1, 80.99(7); P1–Rh1–P2, 161.76(2).

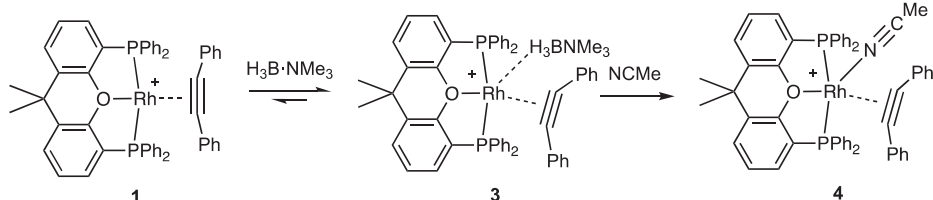
Xantphos environment at 298 K, that suggests a rapid, but reversible, decoordination of the MeCN to the metal center to afford time resolved  $\text{C}_{2v}$  symmetry. Such behavior is mirrored in the NMR data observed for **3** and the kinetic model (Fig. 3).

We propose a catalytic cycle as shown in Scheme 3. Addition of  $\text{H}_3\text{B}\cdot\text{NMe}_3$  to **1** reversibly forms **3**, with the equilibrium biased towards the adduct and away from **1**. B–H activation to form a boryl hydride, **A**, is followed by turnover limiting irreversible [16] alkyne insertion into the Rh–H bond to give the vinylboryl species **B**. While this is consistent with the measured KIE of 1.4 [17], we cannot discount an alternative rapid and reversible [6,18] B–H activation followed by turnover limiting irreversible alkyne insertion into the Rh–B bond [19]. Equilibrium isotope effects would certainly be operating in both these processes, making a definitive interpretation of the measured KIE more difficult [20,21]. While the precise nature of the steps involved in the turnover limiting manifold (i.e. **3** to **B**) remain to be delineated, subsequent reductive coupling forms **C**, in which the product, **2**, can then be rapidly displaced by alkyne to reform **1**. As addition of **2** to **1** does not result in the observation of a new species, and there is no product inhibition, we propose this process is fast and essentially irreversible.

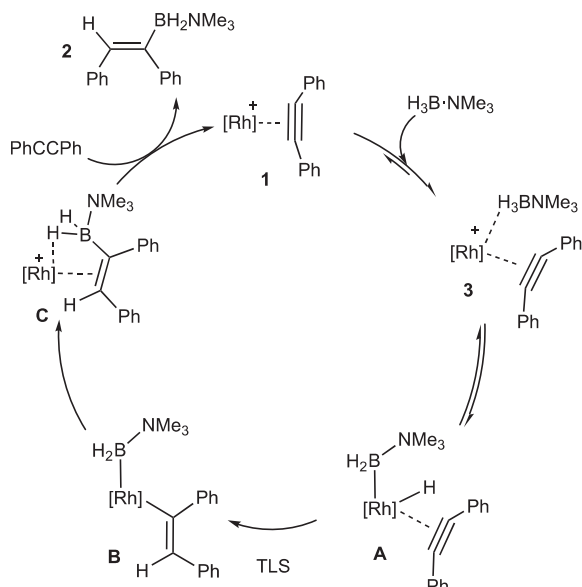
In conclusion we report a *cis*-hydroboration of diphenylacetylene using  $\text{H}_3\text{B}\cdot\text{NMe}_3$  to provide the vinyl borane,  $\text{PhCH}=\text{CPh}(\text{BH}_2\cdot\text{NMe}_3)$ . A detailed kinetics analysis reveals the essential elements of the mechanism, that follows a saturation-kinetics model for amine–borane binding. While the current substrate scope is limited to one alkyne (diphenylacetylene), the elementary steps revealed are relevant to other process involving amine–borane activation, such as dehydropolymerization [22], and we suggest our observations may be helpful in helping delineate these significantly more complex processes.

### 3. Experimental

All manipulations, unless otherwise stated, were performed under an atmosphere of argon using standard Schlenk and glovebox techniques. Glassware was oven dried at 130 °C overnight and flamed under vacuum prior to use.  $\text{CH}_2\text{Cl}_2$ , MeCN,  $\text{Et}_2\text{O}$ , pentane and hexane were dried using a Grubbs-type solvent purification system (MBraun SPS-800) and degassed by successive freeze–pump–thaw cycles. 1,2- $\text{C}_6\text{H}_4\text{F}_2$



**Scheme 2.** Suggested resting state, **3**, and reaction with MeCN to form complex **4**.  $[\text{BAR}_4^+]$  anions not shown.



**Scheme 3.** Suggested mechanism for the hydroboration of  $\text{PhC}\equiv\text{CPh}$  by  $\text{H}_3\text{B}\cdot\text{NMe}_3$  promoted by **1**.

(pretreated with alumina) and  $\text{CD}_2\text{Cl}_2$  were dried over  $\text{CaH}_2$ , vacuum distilled and stored over 3 Å molecular sieves. NMR spectra were recorded on Varian Unity 500 MHz, Bruker AVIII500, Bruker DPX250 or Bruker AVIII400 spectrometers at room temperature, unless otherwise stated. Residual protio solvent was used as a reference for  $^1\text{H}$  NMR spectra in deuterated solvent samples. For 1,2- $\text{C}_6\text{H}_4\text{F}_2$  solvent the spectrometer was pre-locked and shimmed to a sample containing 25%  $\text{C}_6\text{D}_6$  and 75% 1,2- $\text{C}_6\text{H}_4\text{F}_2$  and referenced to the center of the downfield solvent multiplet ( $\delta$  7.07 or 7.11, respectively).  $^{31}\text{P}\{^1\text{H}\}$  and  $^{11}\text{B}$  NMR spectra were referenced externally against 85%  $\text{H}_3\text{PO}_4$  and  $\text{BF}_3\cdot\text{OEt}_2$ , respectively. Chemical shifts are quoted in ppm. Coupling constants are quoted in Hz. Electrospray ionization mass spectrometry (ESI-MS) data were recorded using a Bruker MicroTOF instrument directly connected to a modified Innovative Technology glovebox [23]. Samples were diluted to a concentration of approximately  $1 \times 10^{-6}$  M before analysis. Elemental microanalyses were performed by Stephen Boyer at London Metropolitan University (UK). The starting materials  $\text{D}_3\text{B}\cdot\text{NMe}_3$  [24], and *mer*- $[\text{Rh}(\kappa^3\text{-P},\text{O},\text{P-Xantphos})(\eta^2\text{-PhC}\equiv\text{CPh})][\text{BAr}_4^F]$ , **1** [8], were prepared by literature methods or variations thereof.  $\text{H}_3\text{B}\cdot\text{NMe}_3$  was purchased from Boron Specialties and sublimed twice prior to use ( $5 \times 10^{-2}$  mbar, 298 K). Diphenylacetylene was purchased from Aldrich and used without further purification. Structure determinations were collected on an Oxford Diffraction/Agilent SuperNova diffractometer with Cu-K $\alpha$  radiation ( $\lambda = 1.54184$  Å) equipped with nitrogen gas Oxford Cryosystems Cryostream unit [25]. Diffraction data were reduced and processed using CrysAlisPro package [26]. The structures were solved using SHELXT [27] and refined to convergence on  $F^2$  and against all independent reflections by full-matrix least-squares using SHELXL [28] (version 2018/3) in combination with the GUI OLEX2 [29] program. All non-hydrogen atoms were refined anisotropically and hydrogen atoms were geometrically placed unless otherwise stated and allowed to ride on their parent atoms.  $\text{CF}_3$  groups on the  $[\text{BAr}_4^F]^-$  anion were necessarily modelled as disordered over two main domains, and restrained to maintain sensible geometries. Full crystallographic data have been deposited with the CCDC as 1887954 (2) and 1887953 (4). These data can be obtained free of charge from the Cambridge Crystallographic Data Centre via [http://optimized.ccdc.cam.ac.uk/data\\_request/cif](http://optimized.ccdc.cam.ac.uk/data_request/cif).

**Synthesis of 2:** To a J. Young's ampoule containing trimethylamineborane  $\text{H}_3\text{B}\cdot\text{NMe}_3$  (50.0 mg, 0.685 mmol, 1 equiv), diphenylacetylene (134.3 mg, 0.754 mmol, 1.1 equiv) and **1** (5.90 mg, 3.43  $\mu\text{mol}$ , 0.5 mol

%) was added 1 mL 1,2- $\text{C}_6\text{H}_4\text{F}_2$  and the resulting solution was stirred for 2 d at room temperature. The solvent was removed *in vacuo* resulting in an oil which was triturated with pentane to give a colorless solid. The solid was washed with further pentane and recrystallized from  $\text{Et}_2\text{O}$  giving  $\text{PhCH}=\text{CPh}(\text{BH}_2\cdot\text{NMe}_3)$  as colorless crystals. (Yield = 88%, 151 mg).

$^1\text{H}$  NMR (400 MHz,  $\text{CD}_2\text{Cl}_2$ , r.t., ppm):  $\delta$  = 7.24–7.15 (m, 4H, Ar-H), 7.12–6.95 (m, 4H, Ar-H), 6.95–6.89 (m, 2H, Ar-H), 6.80 (s, 1H), 2.42 (s, 9H,  $\text{NMe}_3$ ), 2.40 (br s,  $\text{BH}_2$ , overlapping).

$^{13}\text{C}\{^1\text{H}\}$  NMR (100 MHz,  $\text{CD}_2\text{Cl}_2$ , r.t., ppm):  $\delta$  = 148.5 ( $\text{C}_{\text{q,Ar}}$ ), 140.4 ( $\text{C}_{\text{q,Ar}}$ ), 136.7 ( $\text{C}_{\text{vinyl-H}}$ ), 129.6 ( $\text{C}_{\text{Ar-H}}$ ), 129.1 ( $\text{C}_{\text{Ar-H}}$ ), 128.4 ( $\text{C}_{\text{Ar-H}}$ ), 127.8 ( $\text{C}_{\text{Ar-H}}$ ), 125.6 ( $\text{C}_{\text{Ar-H}}$ ), 125.1 ( $\text{C}_{\text{Ar-H}}$ ), 52.7 ( $\text{NMe}_3$ ) (one C not observed, likely that attached to B).

$^{11}\text{B}\{^1\text{H}\}$  NMR (128 MHz,  $\text{CD}_2\text{Cl}_2$ , r.t., ppm):  $\delta$  = 0.86.

ESI-MS ( $\text{CH}_2\text{Cl}_2$ )  $[\text{C}_{17}\text{H}_{23}\text{BNH}] + \text{H}^+$   $m/z$  = 252.1919 (calc. 252.1918).

**Microanalysis**  $\text{C}_{17}\text{H}_{23}\text{BN}$  (251.18) requires: C 81.29, H 8.83, N 5.58; found: 81.17, H 8.96, N 5.59.

**Synthesis of 4:** To a J. Young's crystallization tube containing **1** (30.0 mg, 0.0174 mmol, 1 equiv) was added 0.5 mL of  $\text{CD}_2\text{Cl}_2$  at  $-78^\circ\text{C}$  (dry ice/acetone). MeCN (9  $\mu\text{L}$ , 0.174 mmol, 10 equiv) was added, the reaction mixture was warmed up to room temperature, layered with pentane and stored at room temperature for 3 d giving  $[\text{Rh}(\kappa^3\text{-P},\text{O},\text{P-Xantphos})(\text{NCMe})(\eta^2\text{-PhC}\equiv\text{CPh})][\text{BAr}_4^F]$  as red crystals. (Yield = 78%, 24 mg).

$^1\text{H}$  NMR (400 MHz,  $\text{CD}_2\text{Cl}_2$ , r.t., ppm):  $\delta$  = 7.89 (dd,  $J_1 = 7.7$  Hz,  $J_2 = 1.5$  Hz, 2H, Ar-H), 7.75–7.70 (m, 8H,  $\text{BAr}_4^F$ ), 7.55 (br s, 4H,  $\text{BAr}_4^F$ ), 7.42 (t,  $J = 7.7$  Hz, 2H, Ar-H), 7.39–7.31 (m, 6H, Ar-H), 7.26 (t,  $J = 7.3$  Hz, 4H, Ar-H), 7.22–7.07 (m, 22H, Ar-H), 1.89 (s, 6H, Xantphos  $\text{CH}_3$ ), 1.44 (br s, 3H,  $\text{H}_3\text{CCN}$ ).

$^{11}\text{B}\{^1\text{H}\}$  NMR (128 MHz,  $\text{CD}_2\text{Cl}_2$ , r.t., ppm):  $\delta$  = -6.6 (s,  $\text{BAr}_4^F$ )

$^{31}\text{P}\{^1\text{H}\}$  NMR (162 MHz,  $\text{CD}_2\text{Cl}_2$ , r.t., ppm):  $\delta$  = 27.4 (d,

$^1J_{\text{RhP}} = 115$  Hz).

ESI-MS ( $\text{CH}_2\text{Cl}_2$ ) Positive Ion  $[\text{C}_{55}\text{H}_{45}\text{NOP}_2\text{Rh}]^+$   $m/z$  = 900.21 (calc. 900.20).

**Microanalysis**  $\text{C}_{55}\text{H}_{45}\text{BF}_{24}\text{NOP}_2\text{Rh}$  (1764.04) requires: C 59.24, H 3.26, N 0.79; found: 59.22, H 3.37, N 0.80.

### 3.1. General procedure for kinetic measurements

In a J. Young's high-pressure NMR tube diphenylacetylene,  $\text{H}_3\text{B}\cdot\text{NMe}_3$  and **1** were combined and the tube was sealed. To a second J. Young's high-pressure NMR tube 0.4 mL 1,2- $\text{C}_6\text{H}_4\text{F}_2$  was added and the tube was sealed. Using a J. Young's glass bridge, the solvent was vacuum-transferred from one NMR tube to the other. The NMR spectrometer was set up for the kinetic measurements and the NMR tube was thawed, shaken thoroughly and immediately put in the NMR spectrometer. The reaction progress was monitored by  $^{11}\text{B}$  NMR spectroscopy.

### Acknowledgements

The EPSRC EP/M024210/1 (ASW) and SCG Chemicals Co. Ltd (AJM). With the support of the Erasmus + programme of the European Union (MD). David Ryan is thanked for useful discussions.

### Appendix A. Supplementary data

Supplementary data to this article can be found online at <https://doi.org/10.1016/j.ica.2019.03.032>.

### References

- [1] J. Hartwig, *Organotransition Metal Chemistry: From Bonding to Catalysis*, University Science Books, Sausalito, 2010.
- [2] C.M. Crudden, D. Edwards, *Eur. J. Inorg. Chem.* 2003 (2003) 4695–4712.
- [3] E.C. Neeve, S.J. Geier, I.A.I. Mkhaliid, S.A. Westcott, T.B. Marder, *Chem. Rev.* 116

- (2016) 9091–9161.
- [4] P.V. Ramachandran, M.P. Drolet, A.S. Kulkarni, *Chem. Commun.* 52 (2016) 11897–11900.
- [5] M. Toure, O. Chuzel, J.-L. Parrain, *J. Am. Chem. Soc.* 134 (2012) 17892–17895.
- [6] H.C. Johnson, R. Torrey-Harris, L. Ortega, R. Theron, J.S. McIndoe, A.S. Weller, *Cat. Sci. Technol.* 4 (2014) 3486–3494.
- [7] H.C. Johnson, C.L. McMullin, S.D. Pike, S.A. Macgregor, A.S. Weller, *Angew. Chem. Int. Ed.* 52 (2013) 9776–9780.
- [8] P. Ren, S.D. Pike, I. Pernik, A.S. Weller, M.C. Willis, *Organometallics* 34 (2015) 711–723.
- [9] M. Arambasic, J.F. Hooper, M.C. Willis, *Organic Lett.* 15 (2013) 5162–5165.
- [10] M. Shimoi, T. Watanabe, K. Maeda, D.P. Curran, T. Taniguchi, *Angew. Chem. Int. Ed.* 57 (2018) 9485–9490.
- [11] H. Yoshida, Y. Takemoto, K. Takaki, *J. Asian, Org. Chem.* 3 (2014) 1204–1209.
- [12] C. Lee, L. Xu, M. Singhal, P. Mendes, S. Hoops, J. Pahle, N. Simus, R. Gauges, S. Sahle, U. Kummer, *Bioinformatics* 22 (2006) 3067–3074.
- [13] M. Ingleson, N.J. Patmore, G.D. Ruggiero, C.G. Frost, M.F. Mahon, M.C. Willis, A.S. Weller, *Organometallics* 20 (2001) 4434–4436.
- [14] N. Tsoureas, T. Bevis, C.P. Butts, A. Hamilton, G.R. Owen, *Organometallics* 28 (2009) 5222–5232.
- [15] J. Wagler, A.F. Hill, *Organometallics* 27 (2008) 2350–2353.
- [16] While  $\beta$ -elimination from M-vinyl complexes is rare, it has been proposed to occur slowly on heating at 55 °C. See: C.M. Storey, M.R. Gyton, R.E. Andrew, A.B. Chaplin, *Angew. Chem. Int. Ed.* 57 (2018) 12003–12006.
- [17] J. Barwick-Silk, S. Hardy, M.C. Willis, A.S. Weller, *J. Am. Chem. Soc.* 140 (2018) 7347–7357.
- [18] A.G. Algarra, L.J. Sewell, H.C. Johnson, S.A. Macgregor, A.S. Weller, *Dalton Trans.* 43 (2014) 11118–11128.
- [19] R.T. Baker, J.C. Calabrese, S.A. Westcott, P. Nguyen, T.B. Marder, *J. Am. Chem. Soc.* 115 (1993) 4367–4368.
- [20] E.M. Simmons, J.F. Hartwig, *Angew. Chem. Int. Ed.* 51 (2012) 3066–3072.
- [21] A further scenario is one of a low energy B–H activation, followed by reversible boryl insertion, and a rate-limiting reductive coupling from the resulting Rh(H) (vinylborate) intermediate.
- [22] D. Han, F. Anke, M. Trose, T. Beweries, *Coord. Chem. Rev.* 380 (2019) 260–286.
- [23] A.T. Lubben, J.S. McIndoe, A.S. Weller, *Organometallics* 27 (2008) 3303–3306.
- [24] A.L. Colebatch, B.W. Hawkey-Gilder, G.R. Whittell, N.L. Oldroyd, I. Manners, A.S. Weller, *Chem. Eur. J.* 24 (2018) 5450–5455.
- [25] J. Cosier, A.M.J. Glazer, *J. Appl. Cryst.* 19 (1986) 105–107.
- [26] Agilent, CrysAlis PRO. Agilent Technologies Ltd, Yarnton, Oxfordshire, England, 2014.
- [27] G.M. Sheldrick, *Acta Cryst. Sect. A* 71 (2015) 3–8.
- [28] G.M. Sheldrick, *Acta Cryst. Sect. A* 64 (2008) 112–122.
- [29] O.V. Dolomanov, L.J. Bourhis, R.J. Gildea, J.A.K. Howard, H.J. Puschmann, *Appl. Cryst.* 42 (2009) 339–341.